

Supplement of Solid Earth, 11, 1747–1771, 2020
<https://doi.org/10.5194/se-11-1747-2020-supplement>
© Author(s) 2020. This work is distributed under
the Creative Commons Attribution 4.0 License.



Supplement of

Tracking geothermal anomalies along a crustal fault using (U–Th)/He apatite thermochronology and rare-earth element (REE) analyses: the example of the Têt fault (Pyrenees, France)

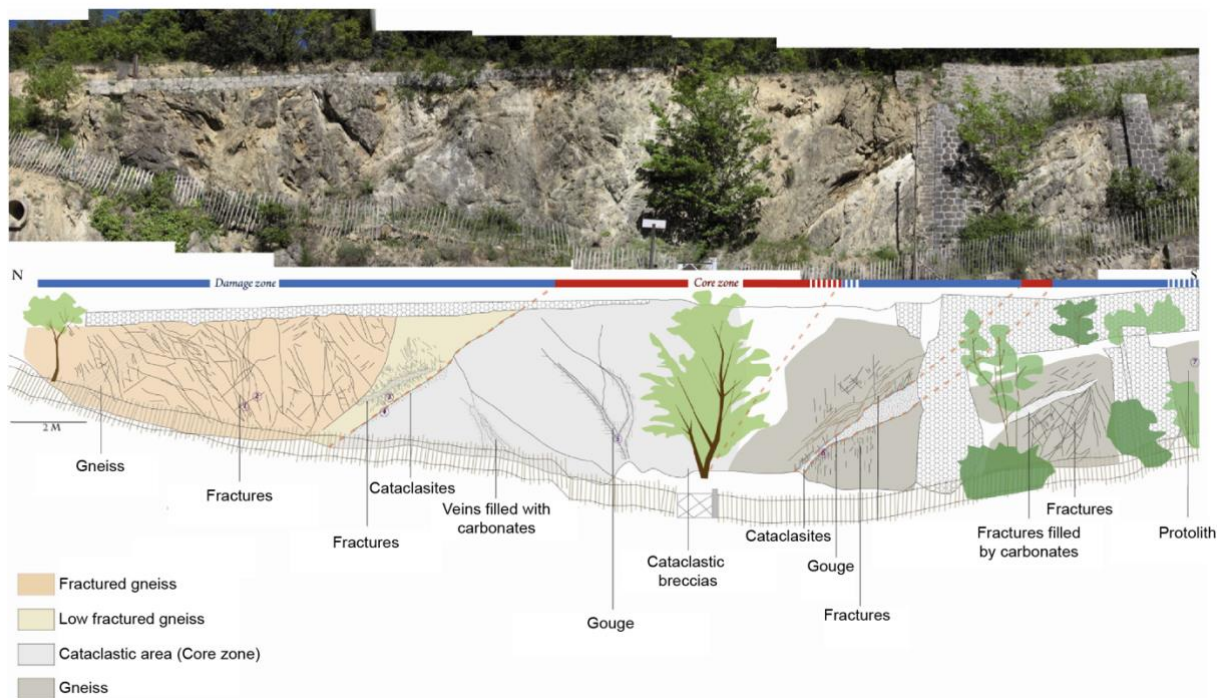
Gaétan Milesi et al.

Correspondence to: Gaétan Milesi (gaetan.milesi@umontpellier.fr)

The copyright of individual parts of the supplement might differ from the CC BY 4.0 License.

Supplement Section

Supplement Section S.1 Fault outcrop



5 **Figure 1. Photo of the Têt fault at Thuès-les-Bains station with interpretation of the fault zone below where Core Zone and Damage zone are distinguished (modified from Martin, 2014). Gneiss lenses are preserved near the fault contact and in the damage zone close to the fault.**

Supplement Section S.2 Hot spring water analyses

10 Table 1. Anion et cation composition of hydrothermal hot springs (ST and PB: Saint-Thomas les Bains hot spring cluster, TB and CA: Thuès hot spring cluster, VB: Vernet-les-Bains,). In bold, data for water potentially mixed with meteoric water from the St-Louis hot spring in Thuès-les-Bains hot spring cluster (from Taillefer, 2017).

Cluster	Llo	Llo	ST		PB	TB			VB		Ca.
			Gd Source	Bar.1	Aig.1	St-Louis	Casc. Amont	Casc. Bas	Du Parc	Vap.	Gr. A - Riv.
Ca	mg/l	2.3	1.5	1.4	1.5	10.1	1.7	1.5	1.5	3	1.4
Mg	mg/l	<0.5	<0.5	<0.5	<0.5	0.7	<0.5	<0.5	<0.5	<0.5	<0.5
Na	mg/l	65.4	55.3	56.4	57	45.8	60.3	60.5	57.2	55.2	60.9
K	mg/l	1.8	1.4	1.3	1.5	1.8	2.4	2.3	1.8	1.9	2.3
NH ₄	mg/l	0.25	0.29	0.32	0.33	<0.05	0.3	0.29	0.2	0.12	0.29
CO ₃	mg/l	21	30	30	33	<10	29	30	25	20	33
HCO ₃	mg/l	29	27	31	29	91	34	32	39	45	31
Cl	mg/l	6.8	8.9	9.2	9.3	8.7	10	9.9	8.4	8.1	7.9
NO ₃	mg/l	<0.5	<0.5	<0.5	<0.5	0.5	<0.5	<0.5	<0.5	<0.5	<0.5
SO ₄	mg/l	51	25.8	25.7	25.7	36.1	28.7	28.3	27.4	37.2	29.5
PO ₄	mg/l	<0.05	<0.05	<0.05	<0.05	<0.05	<0.05	<0.05	<0.05	<0.05	<0.05
NO ₂	mg/l	<0.01	<0.01	<0.01	<0.01	<0.01	<0.01	<0.01	<0.01	<0.01	<0.01
F	mg/l	17.5	7.4	7.7	7.8	5.3	7.9	7.9	6.9	6.7	7
Ag	µg l ⁻¹	<0.01	<0.01	<0.01	<0.01	<0.01	<0.01	<0.01	<0.01	<0.01	<0.01
Al	µg l ⁻¹	6.53	23.5	18.2	24.3	6.15	39.5	60.2	21.3	14.1	31.4
As	µg l ⁻¹	0.07	6.41	5.77	6.6	5.83	3.42	3.67	0.34	1.66	5.78
B	µg l ⁻¹	96.3	109	107	124	221	272	293	301	305	157
Ba	µg l ⁻¹	21.4	12.6	22.3	86.6	6.05	40.2	109	67.5	153	143
Be	µg l ⁻¹	0.01	0.01	<0.01	<0.01	0.04	0.1	<0.01	<0.01	<0.01	<0.01
Cd	µg l ⁻¹	0.01	<0.01	<0.01	<0.01	<0.01	<0.01	<0.01	<0.01	<0.01	<0.01
Cr	µg l ⁻¹	<0.05	<0.05	<0.05	<0.05	<0.05	<0.05	<0.05	<0.05	<0.05	<0.05
Cu	µg l ⁻¹	<0.1	<0.1	<0.1	<0.1	0.7	<0.1	<0.1	<0.1	<0.1	<0.1
Fe	µg l ⁻¹	<0.02	<0.02	<0.02	<0.02	<0.02	<0.02	<0.02	<0.02	<0.02	<0.02
Li	µg l ⁻¹	95.3	78	80.1	81.3	71.1	87.7	87.7	69.5	75	93.9
Mn	µg l ⁻¹	0.15	0.11	<0.1	<0.1	0.1	<0.1	<0.1	<0.1	<0.1	<0.1
Ni	µg l ⁻¹	<0.1	<0.1	<0.1	<0.1	<0.1	<0.1	<0.1	<0.1	<0.1	<0.1
Pb	µg l ⁻¹	<0.05	<0.05	<0.05	<0.05	0.2	<0.05	<0.05	<0.05	<0.05	<0.05
SiO ₂	µg l ⁻¹	55.6	75.3	72.3	79.1	71.8	92.2	92.7	72.7	70.2	91.2
Sr	µg l ⁻¹	67	21.9	25.8	20.5	57.8	29.8	28.8	43	75.9	31.9
Zn	µg l ⁻¹	0.87	1.91	1.32	3.53	3.19	1.5	2.65	1.51	2.98	2.86

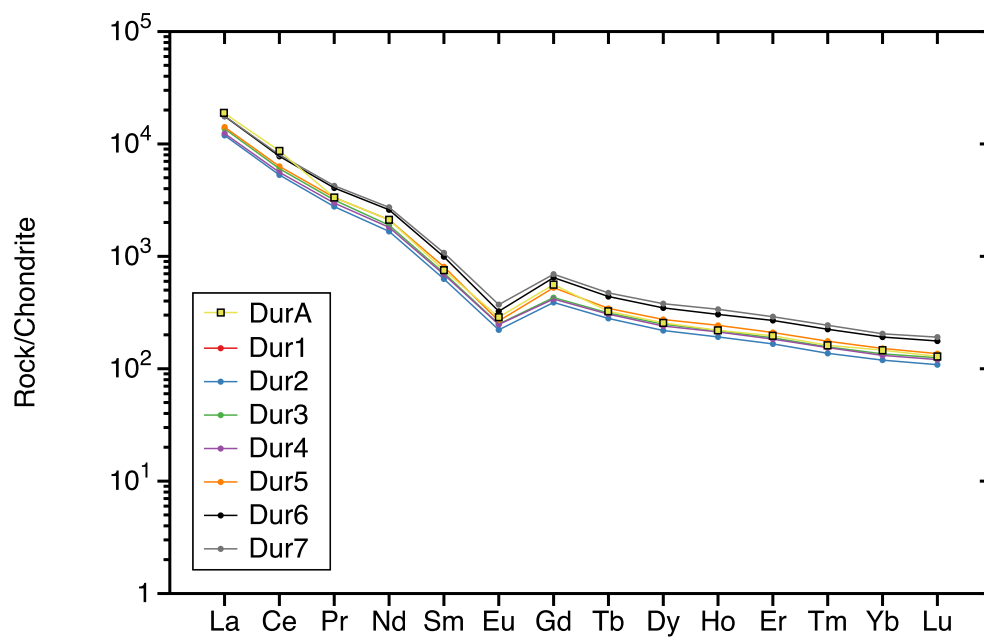
Supplement Section S.3 Apatite grains



15

Figure 2. Photographs of apatite grains selected for (U-Th)/He analyses taken under binocular. Sample name is indicated on the upper left corner. Note that apatites are basically well preserved in the damage zone and outside damage zone.

Supplement Section S.4 REE analyses



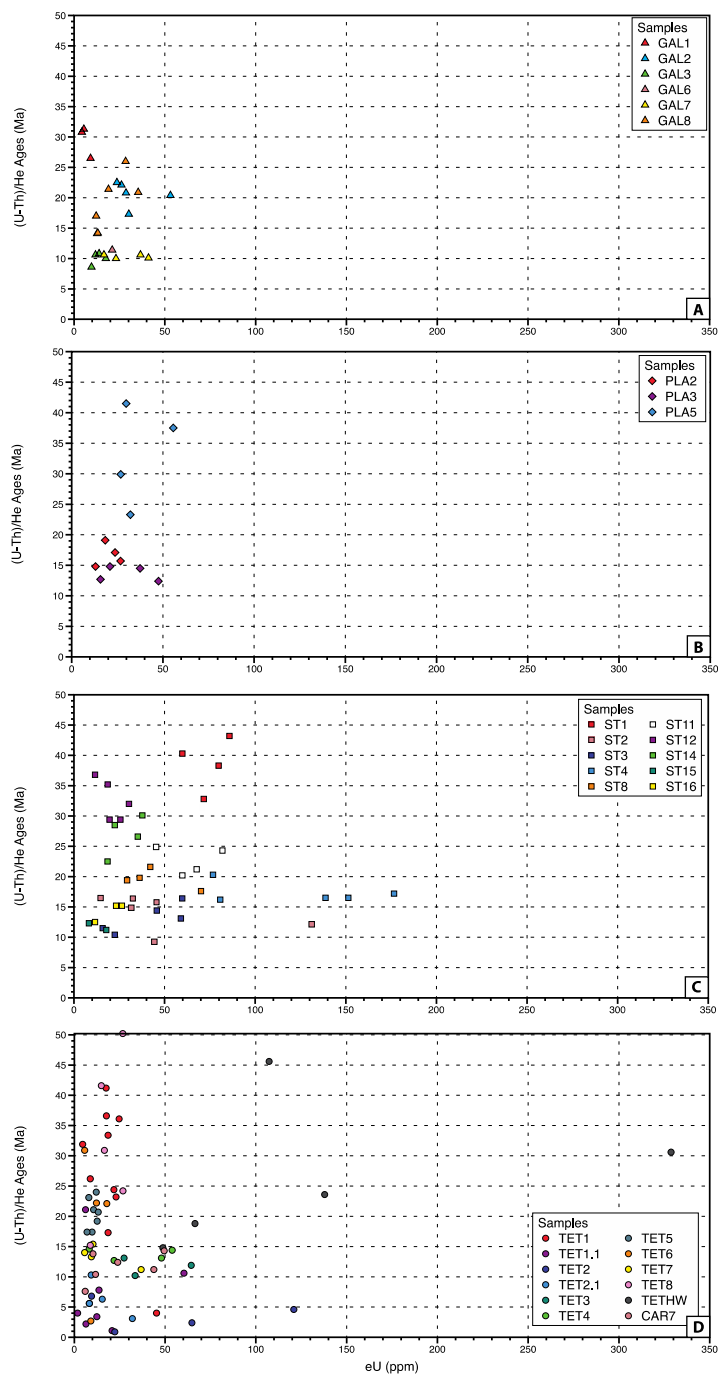
20

Figure 3. REE patterns for Durango apatite standards, consistent with DurA analysis of Chew et al. (2016).

Table 2. Chondrite normalised REE content of dated apatite grains according to Sun and McDonough (1989).

		Footwall samples															
	Name	AHe ages	La	Ce	Pr	Nd	Sm	Eu	Gd	Tb	Dy	Ho	Er	Tm	Yb	Lu	ΣREE
TET Profile	TET1-2	23.2	132.0	462.8	85.7	489.5	233.5	7.7	381.9	72.2	443.0	76.7	167.3	20.0	99.5	12.0	2683.8
	TET1-3	36.1	178.4	582.3	105.1	583.2	283.5	8.8	457.8	85.5	502.9	81.2	170.6	19.8	93.5	11.3	3161.9
	TET1-4	41.2	100.0	349.7	66.0	383.8	186.4	6.5	313.6	57.7	338.8	55.8	115.9	13.6	65.8	7.9	2061.5
	TET1.1-1	4.0	19.6	67.4	13.1	76.9	38.2	2.4	62.8	11.5	67.0	10.8	22.7	2.6	13.1	1.6	409.6
	TET1.1-2	2.2	31.7	103.4	19.6	112.4	54.4	3.4	85.6	15.6	91.3	15.2	32.2	3.8	19.8	2.3	590.8
	TET1.1-4	21.1	67.5	241.6	42.4	233.0	108.0	3.1	168.4	31.6	188.9	31.1	64.9	7.8	40.6	4.6	1233.6
	TET1.1-11	3.4	46.8	160.4	30.5	175.4	85.0	5.0	136.7	24.6	141.3	23.6	52.4	6.2	33.3	3.9	925.2
	TET1.1-12	1.1	54.7	181.8	34.4	202.7	96.3	5.4	157.2	28.4	170.9	30.5	68.5	8.1	41.4	5.0	1085.1
	TET1.1-13	10.6	127.3	411.1	74.6	413.5	193.8	12.0	297.5	54.6	325.0	57.0	127.3	15.9	86.4	10.2	2206.2
	TET2.1-1	10.3	28.9	101.8	20.5	125.8	43.2	4.9	55.3	7.7	44.4	8.9	22.1	2.8	15.8	2.3	484.4
	TET2.1-2	3.1	15.0	53.6	10.5	62.7	24.9	1.5	36.3	5.7	33.1	6.1	13.5	1.5	7.4	1.0	272.8
	TET2.1-4	5.6	26.4	83.8	16.0	97.2	33.1	3.3	42.8	6.4	38.5	7.8	20.1	2.7	15.6	2.2	395.9
TET2.1-11	5.6	26.6	83.6	16.5	103.5	39.0	4.5	51.5	7.6	45.3	9.4	25.2	3.5	18.7	2.8	437.5	
TET2.1-12	6.3	33.7	111.8	22.1	140.6	54.7	5.3	75.0	11.3	70.9	14.9	39.4	5.4	32.1	4.5	621.7	
TETS-2	23.1	91.6	307.0	54.2	295.3	137.5	3.9	213.6	39.6	233.7	38.3	80.6	9.4	48.4	5.7	1558.8	
TETS-4	20.7	108.3	361.4	65.2	353.5	164.0	4.9	258.8	49.4	296.2	49.3	105.0	12.4	64.1	7.7	1900.1	
CAR sample	CAR7-1	11.2	102.0	354.1	66.1	373.9	172.9	9.8	272.0	50.3	301.7	51.8	113.6	13.9	70.7	8.6	1961.4
	CAR7-2	7.6	31.1	109.4	20.7	123.5	38.7	4.1	35.9	17.0	100.4	16.9	35.8	4.1	19.8	2.4	639.0
	CAR7-3	10.4	47.2	144.9	25.9	147.1	68.9	3.8	107.5	19.6	117.1	19.9	44.4	5.5	29.6	3.6	785.0
	CAR7-4	12.4	111.4	370.8	67.9	387.9	175.9	12.6	283.5	51.6	310.5	53.8	119.0	14.1	72.7	9.0	2040.7
	CAR7-5	13.8	67.6	223.5	41.0	236.3	108.6	6.6	170.3	30.5	179.1	30.3	63.7	7.0	32.7	3.9	1201.1
	CAR7-6	14.3	131.4	453.4	82.5	462.0	218.4	7.9	338.1	62.8	374.2	64.9	144.2	17.9	98.6	11.5	2467.7
GAL Profile	GAL7-1	10.6	52.3	153.6	27.1	152.6	41.6	6.1	55.4	7.2	41.8	8.6	22.2	3.1	20.1	3.6	595.4
	GAL7-2	10.0	239.8	675.5	108.8	554.9	149.2	13.7	177.4	25.0	145.9	29.8	73.4	9.7	56.3	8.7	2268.1
	GAL7-3	10.6	181.1	507.9	80.6	413.0	104.8	15.8	122.9	16.2	94.1	19.7	52.1	7.3	47.4	8.3	1671.3
	GAL7-4	10.1	86.8	256.6	45.9	280.3	142.2	9.2	321.5	65.2	478.0	108.2	299.8	43.6	272.8	36.7	2446.8
GAL Profile	GAL3-1	14.1	90.0	252.2	43.9	246.0	68.4	9.2	125.0	14.5	79.5	15.8	33.5	4.5	26.7	4.3	1013.4
	GAL3-2	10.8	58.5	162.8	28.0	158.4	44.4	5.5	84.1	9.3	48.4	9.4	18.9	2.5	13.3	2.2	645.7
	GAL3-3	8.6	120.8	307.9	49.5	259.2	66.8	8.2	124.7	13.5	71.7	14.1	30.0	4.0	21.2	3.6	1095.3
	GAL3-4	10.6	116.0	297.8	49.0	258.1	65.2	9.1	113.6	13.1	70.6	14.2	29.3	3.9	23.4	3.8	1067.1
ST Profile	ST15-1	11.2	12.6	41.7	9.7	81.9	69.9	4.2	178.4	37.5	278.7	63.6	169.4	22.2	126.1	16.1	1111.9
	ST15-2	12.3	40.2	139.5	26.4	155.4	72.7	2.7	108.5	18.8	109.1	19.3	44.3	6.2	38.5	4.7	786.3
	ST16-1	12.5	44.4	157.2	30.8	181.6	92.8	3.3	143.9	26.2	153.4	25.9	56.2	6.8	35.9	4.3	962.8
	ST16-2	15.2	64.4	236.4	46.4	275.0	140.1	5.0	212.4	39.3	234.7	39.7	88.5	11.0	58.1	6.8	1457.9
	ST16-3	15.2	81.5	290.8	56.4	341.0	160.8	6.0	240.6	43.2	263.7	47.3	110.6	15.1	93.7	11.6	1762.1
	ST2-1	16.4	63.9	213.0	38.9	219.5	98.3	4.5	134.1	24.2	150.1	27.4	66.2	8.5	47.6	5.5	1101.8
	ST2-2	14.8	117.2	407.2	79.3	460.8	203.4	8.2	274.6	48.8	305.7	58.0	140.7	18.6	101.0	11.9	2235.6
	ST2-3	12.1	2569.6	3300.4	331.0	1307.4	388.3	22.4	539.0	96.5	598.9	112.9	269.0	33.6	174.2	20.8	9763.8
	ST2-4	9.2	1294.2	1576.7	147.5	563.5	143.5	9.1	171.0	29.0	179.3	33.9	84.4	11.3	62.7	7.5	16418.1
	ST2-5	15.7	240.6	833.6	156.3	870.9	334.6	13.2	415.8	73.3	465.5	89.6	228.6	31.6	184.7	22.2	3960.5
	ST2-6	16.3	137.5	487.4	93.1	534.7	228.5	9.1	305.3	53.5	338.1	62.0	151.7	20.4	109.6	13.1	2544.1
	ST4-1	16.5	146.7	464.1	82.0	410.7	205.3	11.1	316.9	64.0	367.0	58.1	124.6	15.2	78.5	9.1	2353.2
ST4-2	17.2	242.6	751.6	126.3	624.1	305.6	15.5	482.1	99.8	577.3	93.1	204.6	25.4	136.4	15.8	3700.3	
ST4-3	16.5	181.7	578.2	99.1	487.5	249.7	12.3	384.7	79.4	454.3	71.8	153.4	19.0	99.1	11.4	2881.9	
ST4-4	16.2	151.0	474.2	80.9	402.1	203.6	10.7	317.6	64.1	365.3	56.8	122.1	14.9	76.6	9.0	2349.0	
ST4-5	20.3	108.2	349.8	60.5	303.9	157.1	8.3	240.3	48.9	274.4	42.7	89.8	11.0	57.0	6.6	1758.5	
ST8-1	21.6	191.5	626.6	113.1	624.5	306.3	9.9	486.6	93.1	541.5	89.1	189.3	22.6	113.2	13.3	3420.7	
ST8-2	19.8	133.7	475.0	90.6	512.6	252.0	7.2	389.2	74.1	435.8	71.2	150.9	17.8	88.6	10.2	2708.9	
ST8-3	19.4	138.0	477.5	89.1	500.8	245.6	9.4	394.8	75.6	457.4	77.9	167.3	20.1	105.4	12.6	2771.4	
ST8-4	17.6	260.2	884.4	160.9	891.4	431.8	14.1	696.0	132.7	788.5	130.2	274.0	31.8	154.7	18.1	4868.8	
PLA Profile	PLA3-1	12.4	83.4	255.1	47.4	281.2	136.3	4.2	228.4	43.1	286.7	56.5	144.5	20.1	117.7	14.8	1719.5
	PLA3-2	12.7	27.5	92.3	18.6	122.1	66.9	2.0	112.3	20.3	131.8	25.7	64.6	8.9	52.4	6.8	752.2
	PLA3-3	14.8	38.4	123.8	24.3	155.0	81.3	2.4	134.4	24.7	158.4	30.8	76.6	10.5	61.9	8.0	930.3
	PLA3-4	14.5	70.9	237.1	46.4	292.6	157.5	4.6	262.3	48.2	312.7	61.1	152.5	21.1	120.9	15.8	1803.8
PLA2-1	17.1	172.3	596.1	112.2	640.6	329.7	7.7	514.0	94.4	554.8	92.5	199.0	23.8	120.2	14.5	3471.5	
PLA2-2	14.8	105.0	280.8	74.6	447.7	243.5	6.5	381.9	69.2	396.8	65.0	138.3	16.5	82.0	9.8	2417.5	
PLA2-3	19.1	139.0	480.9	94.9	546.2	272.3	7.4	441.1	82.1	488.1	82.6	180.5	21.5	111.2	13.1	2960.8	
PLA2-4	15.7	134.4	484.4	92.0	534.2	287.7	6.0	445.3	81.2	468.6	78.0	168.4	20.0	104.1	12.3	2916.7	
		Hanging wall samples															
	Name	AHe ages	La	Ce	Pr	Nd	Sm	Eu	Gd	Tb	Dy	Ho	Er	Tm	Yb	Lu	ΣREE
TET Profile	TETHW-1	30.6	285.6	998.6	182.6	987.4	471.7	16.8	676.8	131.4	808.0	145.8	365.5	49.3	264.2	32.5	5416.1
	TETHW-2	23.6	447.6	1589.1	273.7	1465.7	644.1	14.9	954.2	183.9	1171.6	216.3	518.0	65.8	339.6	41.7	7926.2
	TETHW-4	45.6	387.5	1352.9	231.7	1248.0	508.2	15.9	773.2	144.2	921.9	176.1	431.5	54.1	276.4	33.8	6555.4
	TETHW-5	14.8	93.3	290.0	52.2	284.0	130.8	6.2	198.7	36.9	228.7	42.2	102.9	13.8	77.4	9.2	1566.4
	ST1-1	40.3	234.0	803.5	138.3	720.1	369.3	12.6	531.4	106.4	633.0	103.2	235.8	32.2	190.7	23.8	4134.2
ST1-2	32.8	156.1	564.2	105.0	576.7	289.7	10.1	414.0	80.5	471.6	76.1	168.0	21.3	115.9	14.2	3063.4	
ST1-3	38.3	257.2	876.6	150.4	796.0	382.7	13.5	551.4	110.2	671.2	112.9</						

Supplement Section S.5 Chemical analyses of apatite



25

Figure 4. (U-Th)/He ages vs. eU ($U+0.235*Th$) for the 4 different profiles: A) Thuès B) Galinès C) St-Thomas D) Planès.

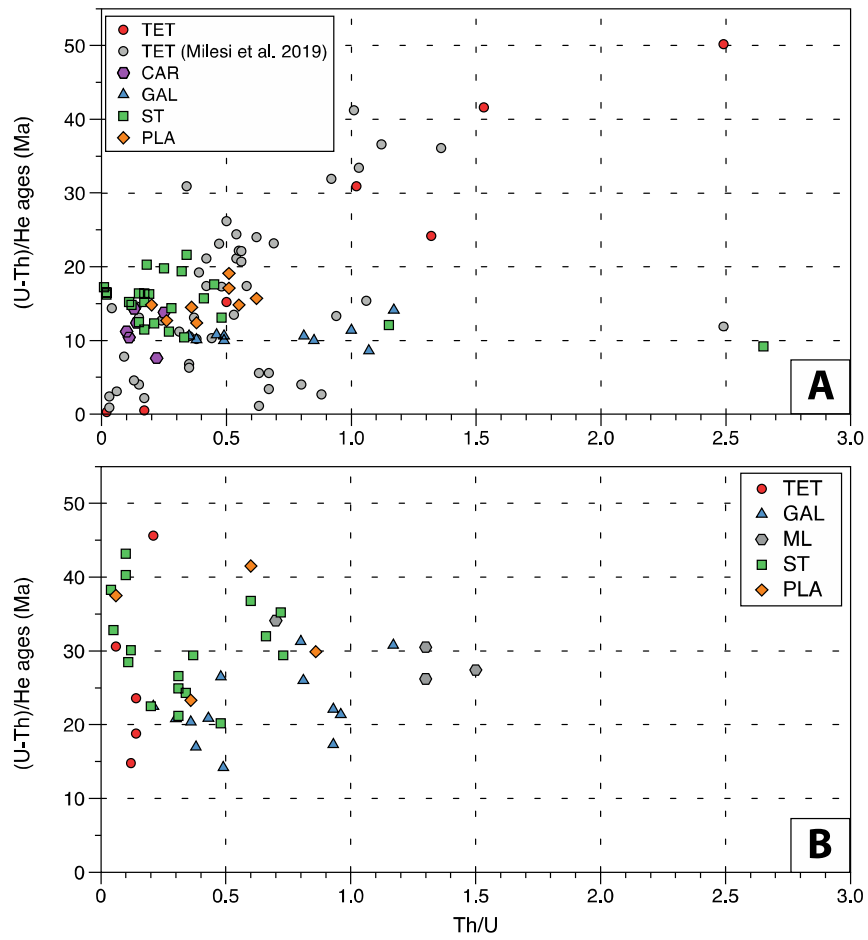


Figure 5. (U-Th)/ages vs. Th/U for A) all the samples from the Têt fault footwall and B) for the Têt fault hanging wall samples.

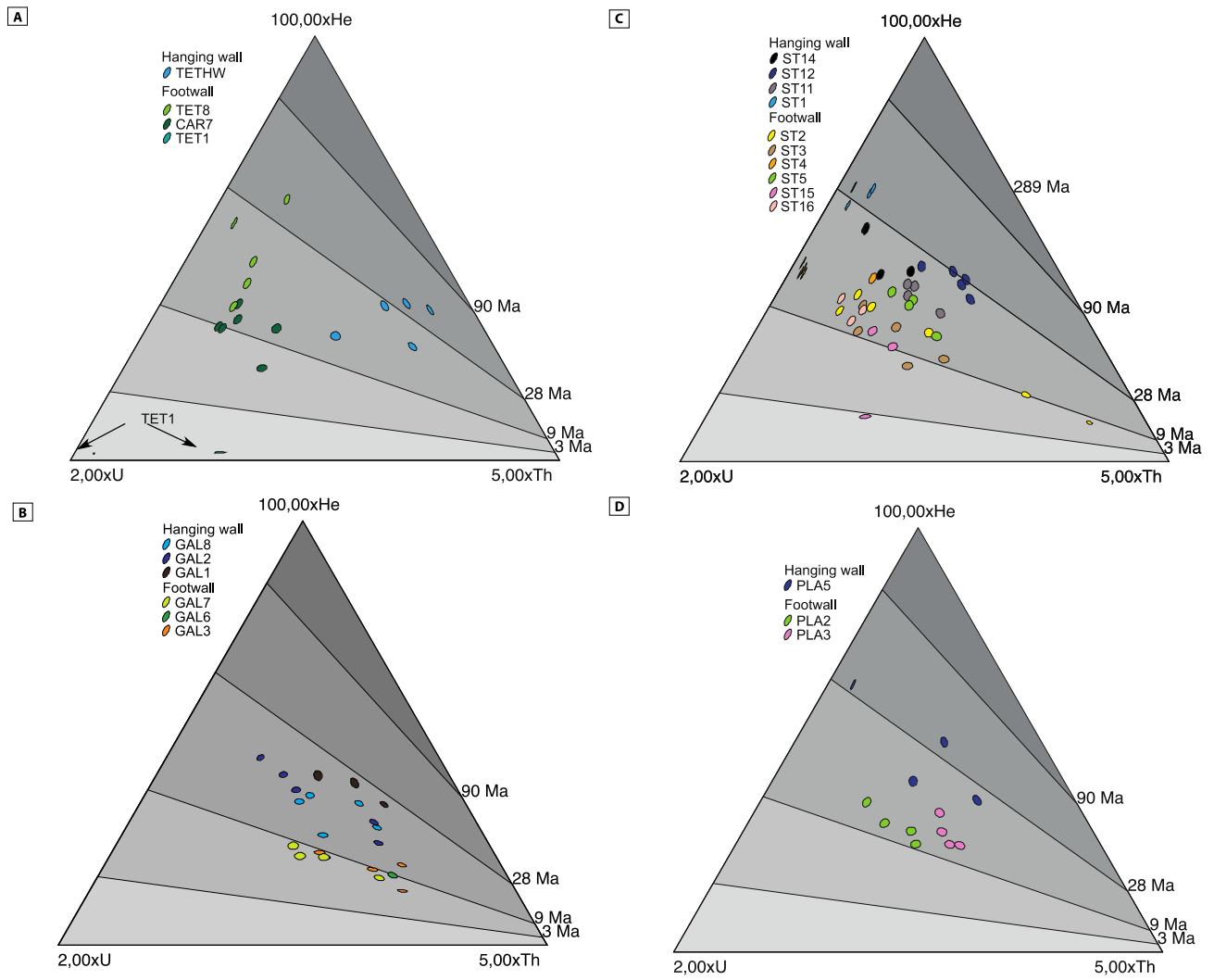


Figure 6. U-Th-He ternary diagrams using Helioplot (Vermeesch, 2010) for the 4 profiles where samples from the Têt fault footwall and hanging wall are distinguished A) Thuès B) Gallinàs C) St-Thomas D) Planès.

Supplement Section S.6 Numerical modelling under QTQt

Table 3. QTQt models parameters for the Têt fault footwall and hanging wall.

QTQt model for the Têt fault footwall

Samples and data used in simulations

AHe data

TET3
TET4
TET5
TET7
GAL3
GAL6
GAL7

AFT data (Maurel et al., 2008)

ZHe data (Maurel et al., 2008)

Data treatment, uncertainties, and other relevant constraints

AHe data

Treatment: Each of the 4 samples was used as a separate constraint in QTQt. Uncorrected

He ages (Ma): Uncorrected He age of each apatite grain

Error (Ma) applied in modelling: the 1σ sample standard deviation

r (μm): equivalent radius of each apatite grain

eU (ppm): eU of each apatite grain

eU zonation: none

Additional geologic information

Assumption

At surface temperature of $15 \pm 10^\circ\text{C}$ by 0 Ma

Motion of Canigou and Carança massif

System and model specific parameters

He kinetic model: Gautheron et al. (2009)

Modelling code: QTQt v.5.7.0

Number of MCMC chain 100000

QTQt model for the Têt fault hanging wall

Samples and data used in simulations

AHe data

ML1
ST14
ST12
GAL2
GAL1

AFT data (Maurel et al., 2008)

ZHe data (Maurel et al., 2008)

Data treatment, uncertainties, and other relevant constraints

AHe data

Treatment: Each of the 4 samples was used as a separate constraint in QTQt. Uncorrected

He ages (Ma): Uncorrected He age of each apatite grain

Error (Ma) applied in modelling: the 1σ sample standard deviation

r (μm): equivalent radius of each apatite grain

eU (ppm): eU of each apatite grain

eU zonation: none

Additional geologic information

Assumption

At surface temperature of $15 \pm 10^\circ\text{C}$ by 0 Ma

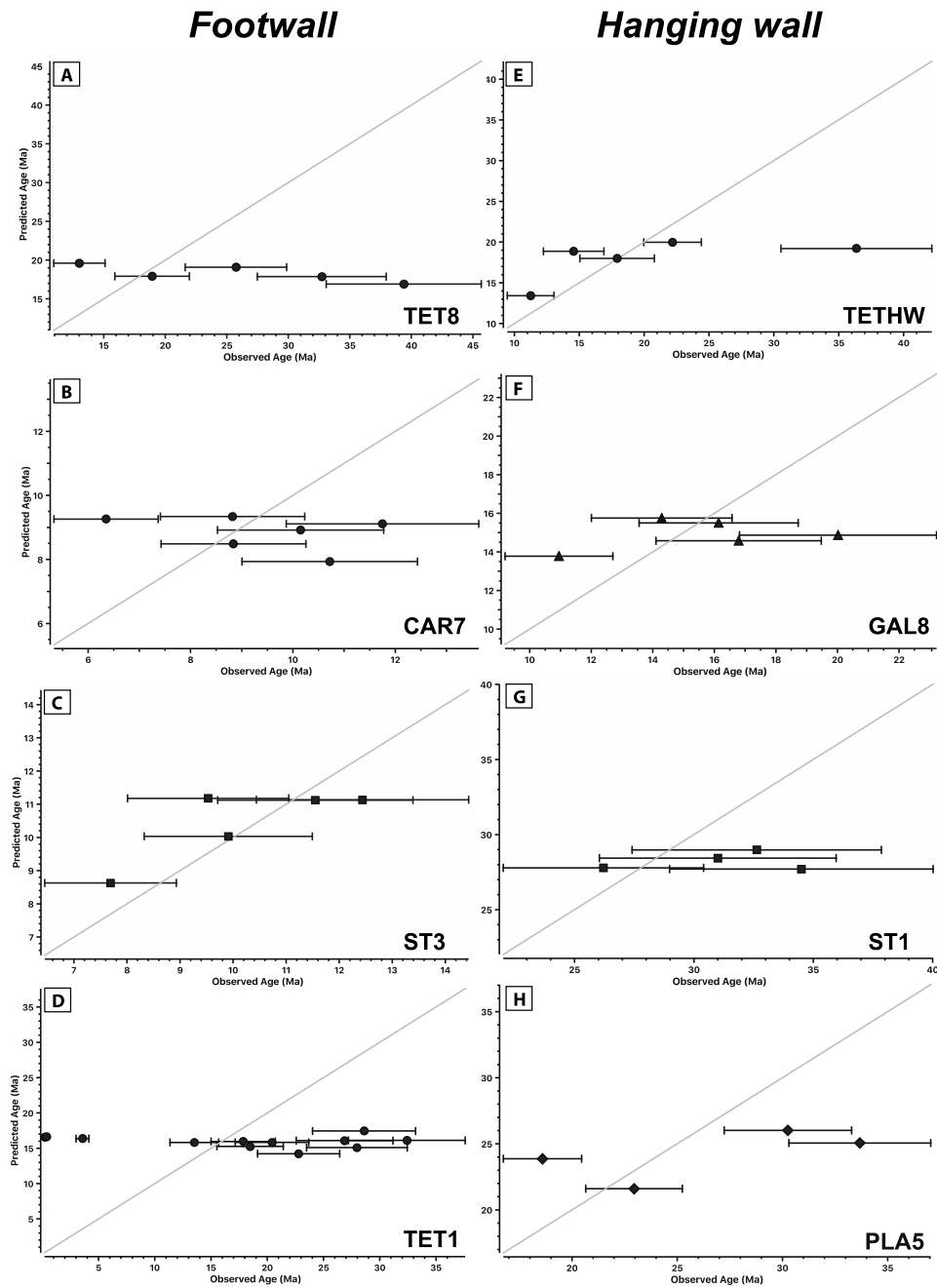
Motion of Mont Louis massif

System and model specific parameters

He kinetic model: Gautheron et al. (2009)

Modelling code: QTQt v.5.7.0

Number of MCMC chain 100000



40 **Figure 7.** Predicted age vs Observed age graph using QTQt (Gallagher, 2012) for samples from the damage zone footwall (A,B,C and D) and hanging wall (E,F,G and H), computed with Gautheron et al. (2009) diffusion model. Modelling parameters are those of Table 3 with AFT and ZHe data from Maurel et al. (2008). For all samples, the weak or the lack of correspondence between observed and predicted ages indicates that no regional cooling history can reasonably explain the AHe age dispersion.

45 References

- Chew, D. M., Babechuk, M. G., Cogné, N., Mark, C., O'Sullivan, G. J., Henrichs, I. A., Doepke, D. and McKenna, C. A.: (LA,Q)-ICPMS trace-element analyses of Durango and McClure Mountain apatite and implications for making natural LA-ICPMS mineral standards, *Chemical Geology*, 435, 35–48, doi:10.1016/j.chemgeo.2016.03.028, 2016.
- Gallagher, K.: Transdimensional inverse thermal history modeling for quantitative thermochronology, *Journal of Geophysical Research: Solid Earth*, 117(B2), n/a-n/a, doi:10.1029/2011JB008825, 2012.
- 50 Gautheron, C., Tassan-Got, L., Barbarand, J. and Pagel, M.: Effect of alpha-damage annealing on apatite (U–Th)/He thermochronology, *Chemical Geology*, 266(3–4), 157–170, doi:10.1016/j.chemgeo.2009.06.001, 2009.
- Martin G. : Analyse des relations entre structure de la faille de la Têt et sources hydrothermales. Master of Science Thesis, Montpellier, 45, 2014.
- 55 Maurel, O., Monié, P., Pik, R., Arnaud, N., Brunel, M. and Jolivet, M.: The Meso-Cenozoic thermo-tectonic evolution of the Eastern Pyrenees: an $^{40}\text{Ar}/^{39}\text{Ar}$ fission track and (U–Th)/He thermochronological study of the Canigou and Mont-Louis massifs, *International Journal of Earth Sciences*, 97(3), 565–584, doi:10.1007/s00531-007-0179-x, 2008.
- Sun, S. S., and McDonough, W. F.: Chemical and isotopic systematics of oceanic basalts: implications for mantle composition and processes. Geological Society, London, Special Publications, 42p, 313–345. <https://doi.org/10.1144/GSL.SP.1989.042.01.19>, 1989.
- 60 Taillefer, A.: Interactions entre tectonique et hydrothermalisme : Rôle de la faille normale de la Têt sur la circulation hydrothermale et la distribution des sources thermales des Pyrénées Orientales., Thesis, Montpellier, 27 October., 242p , 2017.
- Vermeesch, P.: HelioPlot, and the treatment of overdispersed (U–Th–Sm)/He data, *Chemical Geology*, 271(3–4), 108–111, doi:10.1016/j.chemgeo.2010.01.002, 2010.
- 65